Analysis of Structural Phase Transition of Storage Battery Carbon Negative Electrodes Using Synchrotron Radiation and Neutrons

Shigeharu Takagi*1

Abstract

This study used synchrotron radiation and neutron diffraction to carry out operando structural analysis of carbon (graphite) negative electrodes of storage batteries during the charge/discharge process. Low-temperature operando measurement using synchrotron radiation diffraction and neutron diffraction was enabled by the development of a new single-cell measurement tool capable of temperature control. When dQ/dV analysis was performed in accordance with the diffraction pattern, it was found that, at low-temperature, high-rate discharge, structural phase transition of the graphite (i.e., stage structure changes) is inhibited and that transition in multiple phases is facilitated. As a result, it was inferred that this structural transition affects battery low-temperature performance and high-rate discharge performance. In addition, X-ray diffraction (the fundamental parameter method) was used to analyze the crystallite size distribution and quantify the carbon structure, thereby identifying the relationship with battery performance. Furthermore, analysis of the effects on phase transition due to the crystallinity of graphite during charge and discharge found that the multi-phase transition phenomena differed due to the crystallinity of the graphite. This analysis also identified the graphite crystallinity and structural phase transition during charge and discharge, as well as the relationship between these parameters and battery performance.

Keywords: *synchrotron radiation diffraction, neutron diffraction, X-ray diffraction, fundamental parameter method, graphite, crystallite size*

1. Introduction

A number of issues related to storage batteries must be resolved to encourage the widespread adoption of electric vehicles (EVs). These include further increasing capacity, as well as enhancing both low-temperature and high rate charge-discharge characteristics. Understanding the lithium (Li) intercalation and de-intercalation mechanism at the carbon negative electrode of the storage battery is a critical step toward improving these battery performance attributes. To accomplish this objective, it is important to examine structural phase transition states using operando analysis during charge-discharge. Since the structural phase transitions that occur due to temperature change must be analyzed, temperature-controlling tools that can be utilized with synchrotron radiation diffraction and neutron diffraction measurement methodologies are under development. In addition, since recent research has found that the type of carbon used for the storage battery negative electrode causes differences in battery performance, researchers are also working to quantify the physical properties of storage battery carbon negative electrodes. Analysis is focusing on carbon crystallinity as a physical property of carbon that affects battery performance from the standpoint of Li diffusivity.

This article describes the development of new tools capable of low-temperature control (from -10 to 50°C), which enabled operando structural analysis with synchrotron radiation diffraction and neutron diffraction.(1)-(4) This research then applied these developments to identifying how the following factors affected phase transition: the differences under low- and room-temperature conditions, the effects of the charge-discharge rate, and different degrees of carbon crystallinity. Additionally, X-ray diffraction (the fundamental parameter (FP) method(5)) was used to quantify the crystallite size and distribution, and to analyze the relationship between these factors and lithium-ion battery low-temperature performance.(6)

Finally, these results enabled the effects on battery performance at low temperatures and during high rate charge-discharge to be analyzed. This helped to form useful guidelines for the development of next-generation storage battery materials.

*1 Material Engineering Div. No. 2, Advanced R&D and Engineering Company

2. Experimental Methodology

2.1 Phase transition analysis at low temperature (operando structural analysis by neutron diffraction)

For the neutron diffraction measurement, this research used the special environment neutron powder diffractometer (SPICA), located at the BL09 beam port of the Materials and Life Science Experimental Facility (MLF), which is part of the Japan Proton Accelerator Research Complex (J-PARC) in Ibaraki prefecture (**Fig. 1**),[3] and measured neutron diffraction patterns at the QA-bank.

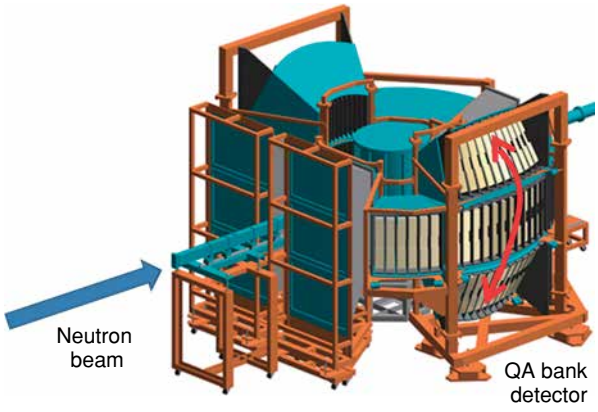

Fig. 1 TOF-Type Neutron Diffractometer (SPICA)

This research utilized polychlorotrifluoroethylene (PCTFE) for the external coating of individual cells. This is a thermoplastic chlorofluoropolymer that contains no hydrogen atoms. This material allowed the analysis to proceed without the use of a deuterium-substituted electrolyte and thoroughly reduced the background noise (reduction rate: 72%). As a result, the signal/noise (S/N) ratio increased and enabled the acquisition of high-quality neutron diffraction data.

The individual cells (four-layer cells) consisted of the following materials. Natural graphite was used for the carbon material, which was coated onto a copper collector foil to create the graphite electrode. Li was used for the counter electrode, and an EC/EMC-system electrolyte (proportion: 3/7 vol%) containing 1 mol/l of $LiPF_6$ in solution was adopted.

The individual cells were subjected to two cycles of pre-treatment (aging) at room temperature (RT). After charging (Li intercalation) at a constant current (CC, 0.1C) and constant voltage (-CV, 0.05 V), the discharge (Li de-intercalation) reactions at 0.05C were analyzed at RT and 0°C. Additionally, the dQ/dv curve was calculated from the charge-discharge curve and the correspondence with the dQ/dV peaks was analyzed.

2.2 Phase transition analysis at low temperature and high-rate discharge (operando structural analysis by synchrotron radiation diffraction)

For the synchrotron radiation diffraction measurement, this research used the BL28XU beamline at the large SPring-8 synchrotron radiation facility under the Research and Development Initiative for Scientific Innovation of New Generation Batteries 2 (RISING 2) initiative.

The individual cells used natural graphite for the carbon material, which was coated onto a copper collector foil to create the graphite electrode, and Li for the counter electrode. An EC/EMC-system electrolyte (proportion: 3/7 vol%) containing 1 mol/l of $LiPF_6$ in solution was adopted in the cells.

The energy of the synchrotron radiation diffraction was set to 25 keV, and a two-dimensional detector (the Pilatus 300K-W manufactured by Rigaku Corporation) was used.

The camera length of the Pilatus 300K-W two-dimensional detector was set to 830 mm. This setting expanded the measurable angular range and improved the angular resolution, enabling the acquisition of X-ray diffraction data containing other than the graphite (002) peak (the main peak).

The individual cells were subjected to two cycles of pre-treatment (aging) at RT. After charging (Li intercalation) at a CC of 0.1C and a -CV of 0.05 V, the discharge (Li de-intercalation) reactions at 0.2C were analyzed at RT and 0°C. Additionally, the dQ/dv curve was calculated from the charge-discharge curve and the correspondence with the dQ/dV peaks was analyzed. The discharge (Li de-intercalation) reactions at 1C were also analyzed at RT.

2.3 Relationship between quantification of carbon structure and battery performance (analysis of crystallite size distribution by X-ray diffraction)

The crystallite sizes and distributions of various carbon (graphite) materials were analyzed using the FP method. Six types of natural carbon (graphite) and four types of artificial graphite were analyzed.

In the FP method, a powder X-ray diffraction pattern simulation is carried out by convoluting machine-derived (i.e., using measurement conditions such as the slit width and sample thickness) profiles with profile shapes derived from the crystallite size and lattice distortion and profile shapes created by the X-ray emission profile. This simulation is used to optimize the crystallite size and lattice distortion parameters, and is capable of obtaining a precise value for the crystallite size distribution by approximation using lognormal distribution or similar techniques. The X-ray diffraction measurement used Cu K(alpha) radiation (0.154 nm).

Coil cells (full cells) were fabricated using the various carbon (graphite) materials described above as the negative electrode active material and a ternary system (NMC) cathode active material. The battery low-temperature and high-rate charge-discharge characteristics were then analyzed using these cells.

The relationship between the physical properties of carbon (graphite) and battery performance was analyzed based on the acquired results.

2.4 Analysis of effect of changes in carbon structure (crystallinity) on phase transition during charge-discharge

Individual cells (aluminum laminated) were fabricated using sample A (natural graphite, high crystallinity) and sample B (artificial graphite, low crystallinity) and the same Li counter electrode as described above. Operando analysis of charge-discharge was also carried out using the same synchrotron radiation diffraction methodology as described above. The energy of the synchrotron radiation diffraction was set to 25 keV, and a two-dimensional detector (the Pilatus 100K manufactured by Rigaku Corporation) was used.

The coin cells and aluminum laminated cells were aged at a predetermined charge-discharge current, and then analyzed at predetermined temperatures and charge-discharge currents.

3. Results and Discussion

3.1 Phase transition analysis at low temperature (operando structural analysis by neutron diffraction)

Fig. 2 shows the developed tool capable of low-temperature control. This tool can control the temperature from low temperatures to RT.

Fig. 2 Developed Temperature-Controlling Tool for Neutron Diffraction

Fig. 3 shows the neutron diffraction results during discharge (i.e., the Li de-intercalation process) with the graphite negative electrode at RT. In the Li de-intercalation process, a clear change can be observed through LiC_6 (d value: around 3.7Å) and LiC_{12} (d value: around 3.5Å) to C (d value: around 3.35 Å). As a result, it was possible to clearly identify the phase transition (i.e., the changes in stage structures) of graphite.

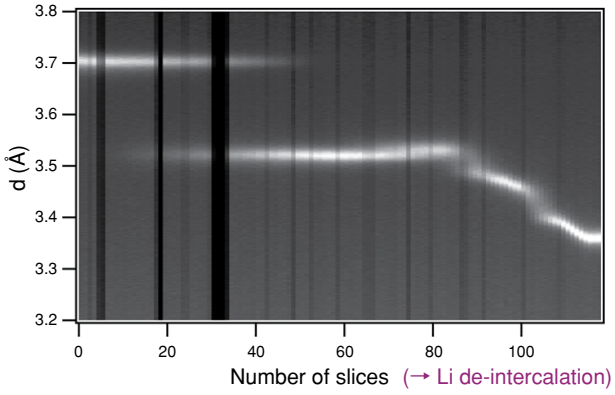

Fig. 3 Neutron Diffraction Pattern in Li De-Intercalation Process (RT, 0.05C)

Fig. 4 shows the dQ/dV curve calculated from the charge-discharge curve. The curve indicates that the phase transition differs at RT and 0°C from stage 2 onward. These results also confirm that operando structural analysis during charge-discharge can be carried out incorporating dQ/dV analysis.

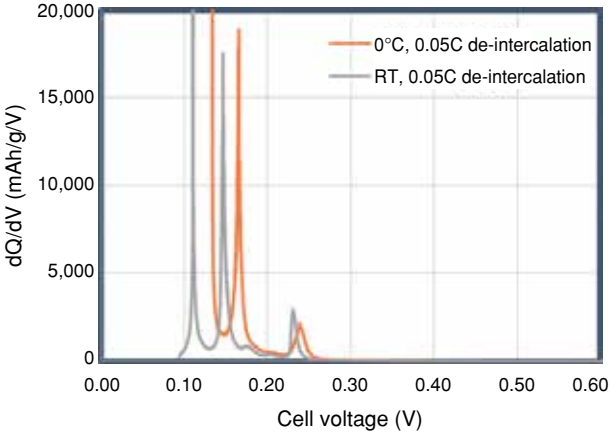

Fig. 4 dQ/dV Curve in Li De-Intercalation Process

Fig. 5 shows an example of the results after isolating the neutron diffraction pattern peaks. The peaks could be clearly isolated even for neutron diffraction patterns expressing multiple phases that include shoulder peaks.

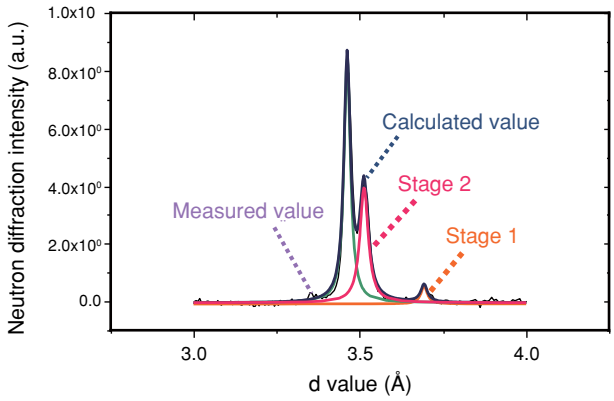

Fig. 5 Peaks Isolated from Neutron Diffraction Pattern (Example)

Neutron diffraction pattern peaks were isolated at state of charge (SOC) intervals of 5% in the Li de-intercalation process. **Figs. 6** and **7** show the state coexistence results of the phases, based on the peak area ratio. In contrast to RT, at which stage structure transition occurred in a single phase, it was found that stage structure transition occurred over multiple phases at 0°C.

These results confirmed the feasibility of operando structural analysis using the developed device configuration for analyzing the phase transition state due to differences in temperature.

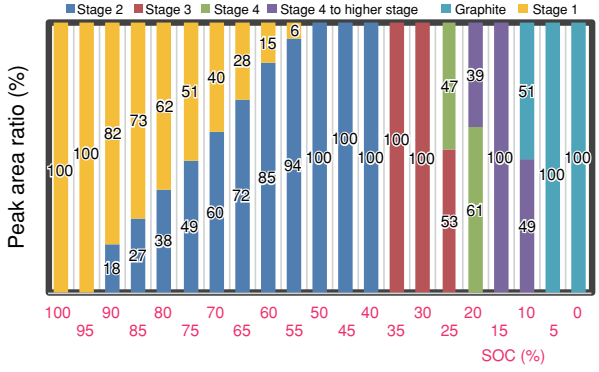

Fig. 6 State of Phase Coexistence in Li De-Intercalation Process (RT, 0.05C)

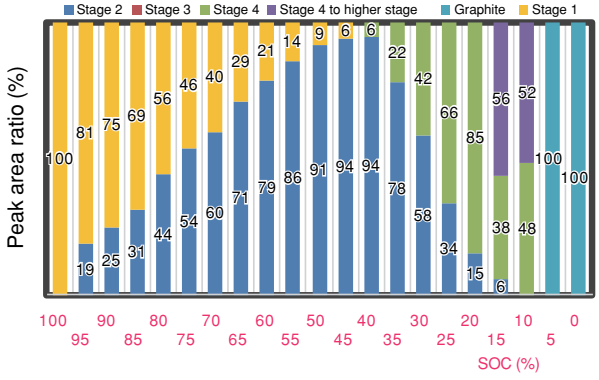

Fig. 7 State of Phase Coexistence in Li De-Intercalation Process (0°C, 0.05C)

From the results described above, it was estimated that structural phase transitions occur over multiple phases during discharge (i.e., the Li de-intercalation process) at low temperatures, and that this phenomenon affects battery low-temperature performance.

3.2 Phase transition analysis at low temperature and high-rate discharge (operando structural analysis by synchrotron radiation diffraction)

Fig. 8 shows the developed tool capable of low-temperature control. This tool can control the temperature from low temperatures to RT.

Fig. 8 Developed Temperature-Controlling Tool for Synchrotron Radiation Diffraction

Fig. 9 shows the synchrotron radiation diffraction results during discharge (i.e., the Li de-intercalation process) with the graphite negative electrode at RT and 0.2C. In the Li de-intercalation process, a clear change can be observed through LiC_6 (2θ: around 7.7°) and LiC_{12} (around 8.1°) to C (around 8.5°). As a result, it was possible to clearly identify the phase transition of graphite.

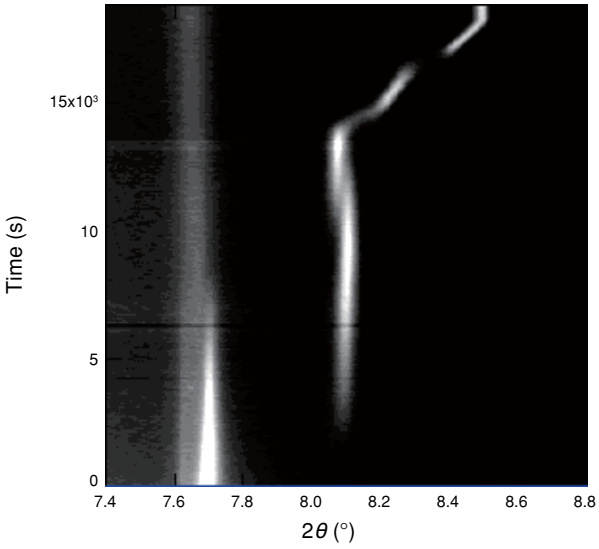

Fig. 9 Synchrotron Radiation Diffraction Pattern in Li De-Intercalation Process (RT, 0.2C)

In the same way as the neutron diffraction analysis, synchrotron radiation diffraction pattern peaks were isolated at SOC intervals of 5% in the Li de-intercalation process. **Figs. 10** and **11** show the state coexistence results of the phases, based on the peak area ratio. Even when the discharge rate was set to 0.2C, stage structure transition occurred in a single phase at RT, but occurred over multiple phases at 0°C.

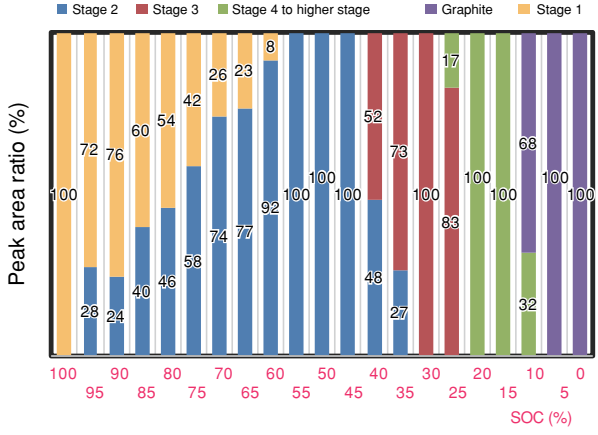

Fig. 10 State of Phase Coexistence in Li De-Intercalation Process (RT, 0.2C)

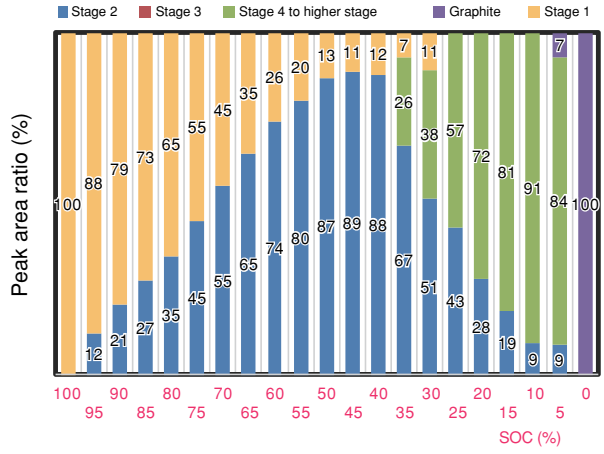

Fig. 11 State of Phase Coexistence in Li De-Intercalation Process (0°C, 0.2C)

Fig. 12 shows the synchrotron radiation diffraction results during discharge (i.e., the Li de-intercalation process) with the graphite negative electrode at RT and 1C. Differences in LiC_{12} (2θ: around 8.1°) behavior can be seen compared with 0.2C and 1C.

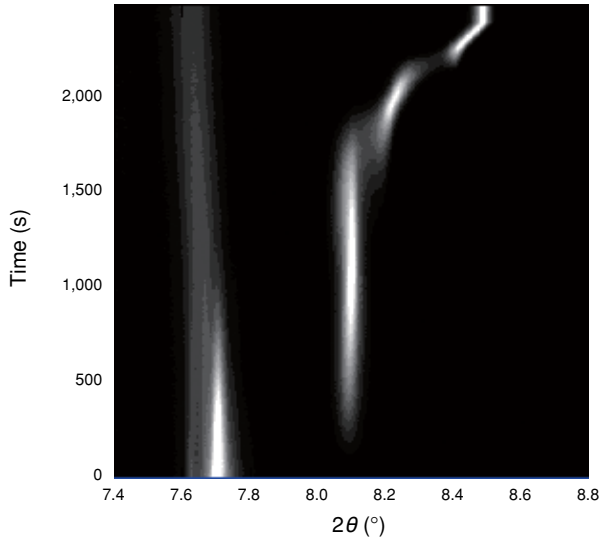

Fig. 12 Synchrotron Radiation Diffraction Pattern in Li De-Intercalation Process (RT, 1C)

Fig. 13 shows an example of the results after isolating the synchrotron radiation diffraction pattern peaks. Analysis was carried out with the exposure time of the detector set to 0.5 s (detection time at 1C). The peaks could be clearly isolated even for synchrotron radiation diffraction patterns expressing multiple phases that include shoulder peaks.

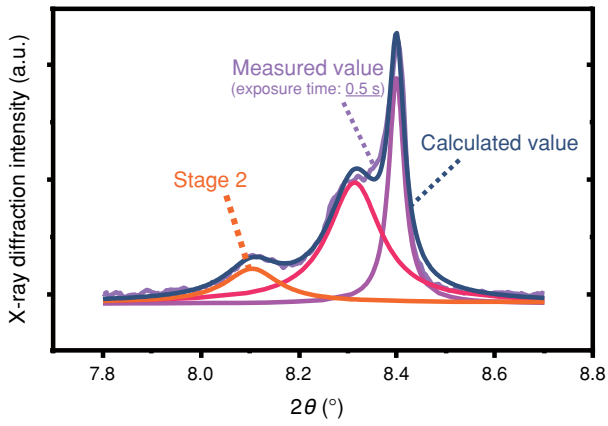

Fig. 13 Peaks Isolated from Synchrotron Radiation Diffraction Pattern (Example)

In the same way as described above, synchrotron radiation diffraction pattern peaks were isolated at SOC intervals of 5% in the Li de-intercalation process at RT and 1C. **Fig. 14** shows the state coexistence results of the phases, based on the peak area ratio. At 0.2C, stage structure transition occurred almost completely in a single phase. However, it was found that stage structure transition occurred over multiple phases at 1C.

These results confirmed the feasibility of operando structural analysis using the developed device configuration for analyzing the phase transition state due to differences in the charge-discharge rate and temperature.

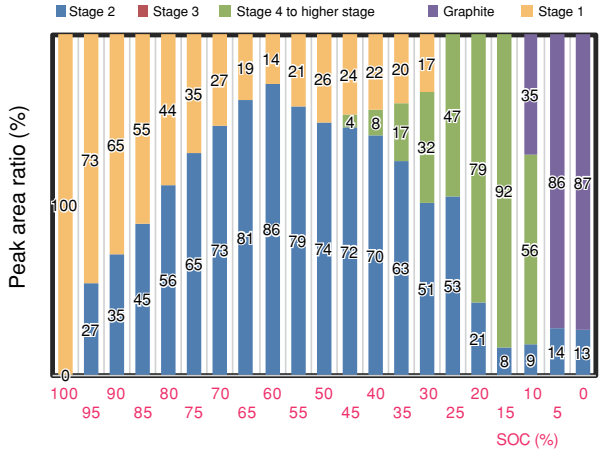

Fig. 14 State of Phase Coexistence in Li De-Intercalation Process (RT, 1C)

From the results described above, it was estimated that stage structure phase transitions occur over multiple phases during discharge (i.e., the Li de-intercalation process) at low temperatures and high discharge rates, and that this phenomenon affects battery performance under these conditions.

3.3 Relationship between quantification of carbon structure and battery performance (analysis of crystallite size distribution by X-ray diffraction)

The carbon crystallite size and distribution were analyzed using the FP method. **Fig. 15** shows an example of the analysis results for crystallite size distribution using the FP method, which were obtained from the X pattern. There is little difference (residual) between the measured and calculated values, indicating the high quality of the calculated results. **Fig. 16** shows the analysis results for crystallite size distribution in these calculations. The crystallite size distribution can be analyzed well at each graphite plane.

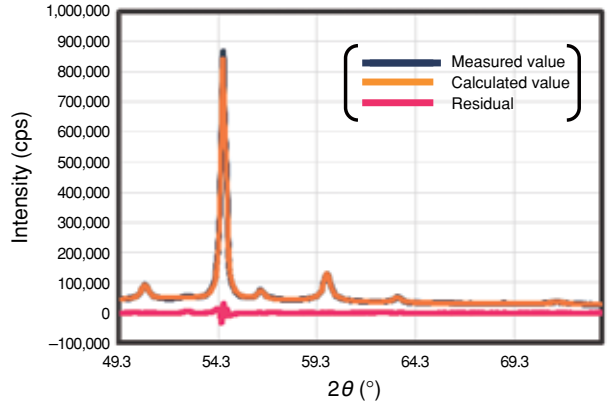

Fig. 15 X-Ray Diffraction Pattern of Carbon

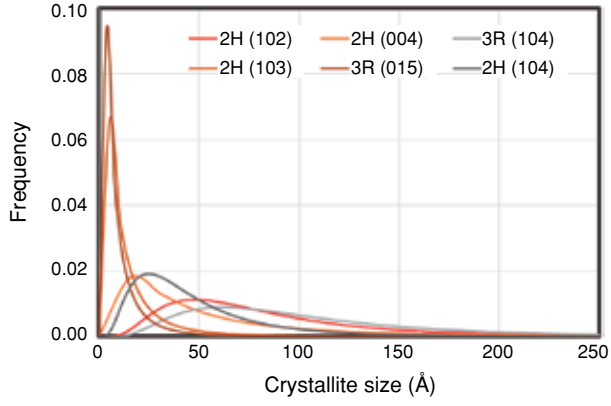

Fig. 16 Crystallite Size Distribution of Graphite

Fig. 17 shows the relationship between the crystallite size distribution of the graphite (102) plane and battery low-temperature characteristics. The discharge capacity (i.e., the specific capacity with respect to the amount of cathode active material) of the full cell at 0°C and 0.5C after charging at 0°C and 0.5C is shown as the low-temperature characteristics. The results indicate that the low-temperature characteristics improve

as the crystallite size and distribution of the graphite (102) plane decreases. The same results were also obtained for the relationship between the crystallite size distribution of the graphite (102) plane and the high-rate discharge characteristics of the battery. The crystallite size distribution of the graphite (102) plane is thought to express the Li diffusivity, considering the diffusion paths of the Li.

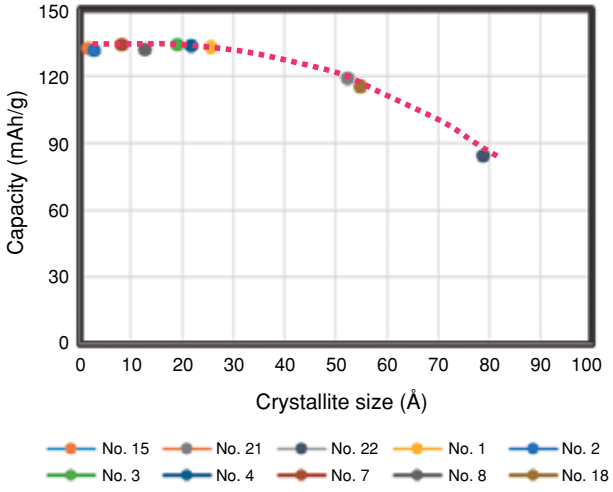

Fig. 17 Relationship between Crystallite Size (Distribution) and Battery Low-Temperature

These results suggest that analyzing the crystallite size and distribution of carbon (graphite) is a feasible way of inferring the low-temperature and high-rate discharge characteristics of a battery.

3.4 Analysis of effect of changes in carbon structure (crystallinity) on phase transition during charge-discharge

Differences in the phase transition during charge-discharge were investigated using sample A (high crystallinity) and sample B (low crystallinity). **Fig. 18** shows the dQ/dV curve in the Li de-intercalation process calculated from the charge-discharge curve. The curve indicates that the phase transition differs between the samples, which have different crystalline properties (i.e., different crystallite sizes), from stage 2 onward.

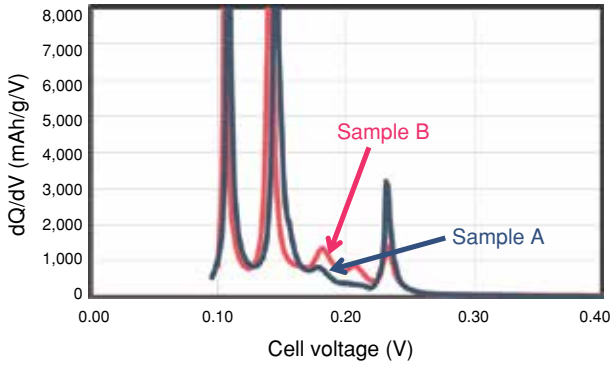

Fig. 18 dQ/dV Curve in Li De-Intercalation Process

In addition, **Figs. 19** and **20** show the phase transition states as analyzed by synchrotron radiation diffraction using sample A (high crystallinity) and sample B (low crystallinity). Here, the transition process to stage 3 is analyzed in detail. The results show that the structure when transitioning to stage 3 differs in accordance with the crystallinity (i.e., the crystallite size). As shown in **Fig. 19**, sample A (high crystallinity) has shoulder peaks and transitions to stage 3 over multiple phases. In contrast, sample B (low crystallinity) has no shoulder peaks in the transition process to stage 3, and the phase transition occurs almost completely in a single phase.

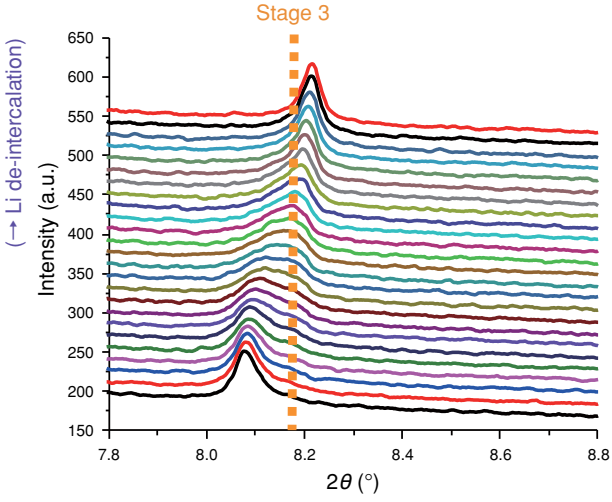

Fig. 19 X-Ray Diffraction Pattern in Stage 3 Transition Process (Sample A, Crystallite Size: Large)

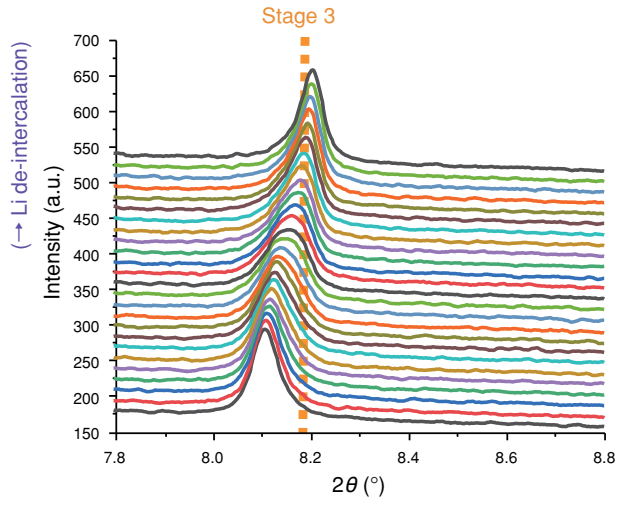

Fig. 20 X-Ray Diffraction Pattern in Stage 3 Transition Process (Sample B, Crystallite Size: Small)

These results suggest that reducing the crystallinity of carbon (graphite) (i.e., reducing the crystallite size) increases the area of edge planes and lattice defects. This facilitates inter-layer transition and the like and boosts Li diffusivity, thereby making transition more likely to occur in a single phase.

4. Conclusions

(1) Synchrotron radiation diffraction and neutron diffraction enabled low-temperature operando structural analysis incorporating dQ/dV to be applied to storage batteries (control is possible from -10 to 50°C).

(2) It was found that transition in multiple phases is more likely to occur at low temperatures than at RT, and at high discharge rates rather than low discharge rates.

(3) The results of the analysis also found that the crystallinity of the carbon (graphite) affects the low-temperature and high-rate discharge characteristics of a battery.

(4) A phenomenon was identified in which differences in carbon (graphite) crystallinity caused differences in phase transition during charge-discharge. A battery reaction mechanism was then identified through which this phenomenon affects low-temperature and high-rate charge-discharge characteristics, thereby facilitating the formation of development guidelines for new materials.

An objective for the future is to use these guidelines in the development of next-generation storage battery materials.

Finally, these research results were obtained as part of the RISING 2 initiative carried out under the auspices of the New Energy and Industrial Technology Development Organization (NEDO). The authors would like to extend their sincere gratitude to everyone involved.

References

(1) S. Takagi et al. “Identification of Physical Properties of Carbon that Affect Battery Performance and Estimation of Performance-Improvement Mechanism Using In-Situ Crystalline Structural Analysis” (in Japanese). *Abstracts of the 58th Battery Symposium in Japan* (2017) p. 1B02.

(2) S. Takagi et al. “Operando Structural Analysis of Graphite Negative Electrode by Synchrotron Radiation Diffraction” (in Japanese). *Abstracts of the 59th Battery Symposium in Japan* (2018) p. 2E14.

(3) M. Yonemura et al. “Development of SPICA, New Dedicated Neutron Powder Diffractometer for Battery Studies.” *Journal of Physics: Conference Series* Vol. 502 (2014).

(4) S. Takagi et al. “Operando Structural Analysis of Graphite Negative Electrode by Neutron Diffraction” (in Japanese). *Abstracts of the 2018 Fall Meeting of the Electrochemical Society of Japan* (2018) p. 1E04.

(5) T. Ida et al. “Diffraction Peak Profiles from Spherical Crystallites with Lognormal Size Distribution.” *Journal of Applied Crystallography* Vol. 36 (2003) pp. 1107-1115.

(6) S. Takagi et al. “Analysis of Carbon Crystallite Size Distribution and its Effects on Battery Low-Temperature Performance” (in Japanese). *Abstracts of the 45th Annual Meeting of the Carbon Society of Japan* (2018) p. 1A06.

Author

S. TAKAGI